RESEARCH ARTICLE

DTI and pathological changes in a rabbit model of radiation injury to the spinal cord after ^{125}I radioactive seed implantation

Xia Cao[1], Le Fang[2], Chuan-yu Cui[3], Shi Gao[4], Tian-wei Wang[5,*]
1 School of Pharmaceutical Sciences, Jilin University, Changchun, Jilin Province, China
2 First Department of Neurology, China-Japan Union Hospital of Jilin University, Changchun, Jilin Province, China
3 Department of MRI, Fourth Hospital, Jilin University, Changchun, Jilin Province, China
4 Department of Nuclear Medicine, China-Japan Union Hospital of Jilin University, Changchun, Jilin Province, China
5 Department of Radiology, China-Japan Union Hospital of Jilin University, Changchun, Jilin Province, China

Funding: *This study was supported by the Science and Technology Development Project Funds of Science and Technology Department of Jilin Province in China, No. 20120724.*

Graphical Abstract

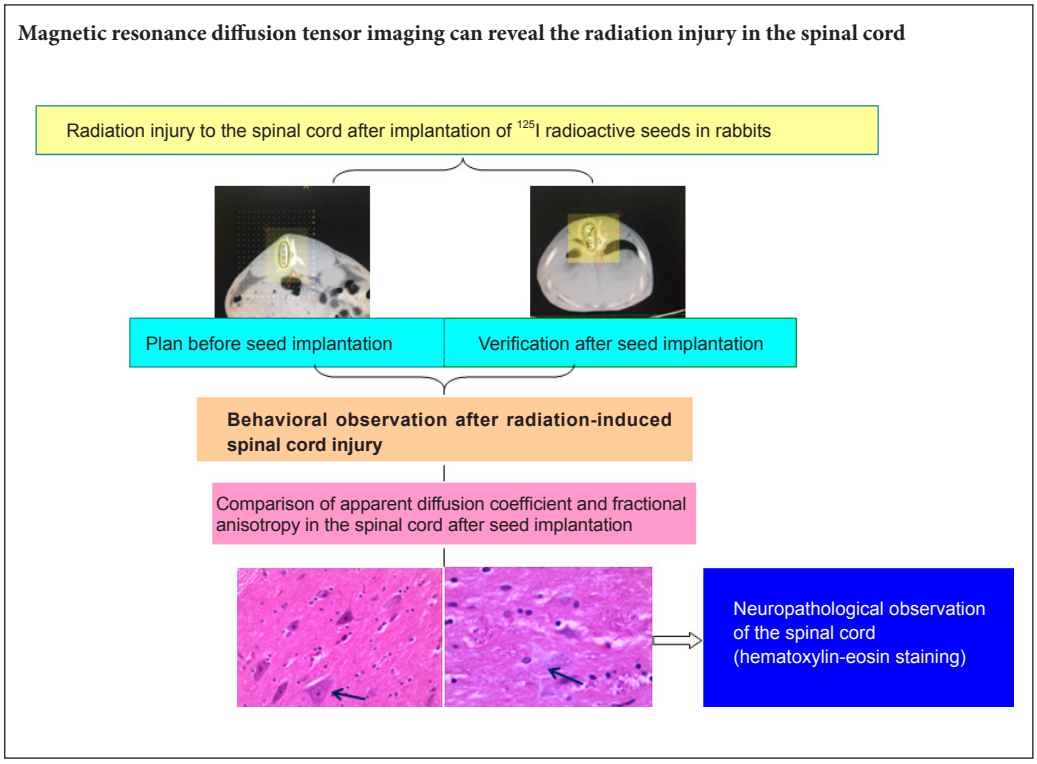

Correspondence to:
Tian-wei Wang, Ph.D., wtw567@sina.com.

orcid:
0000-0002-2187-7691 (Tian-wei Wang)

doi: *10.4103/1673-5374.228758*

Accepted: *2017-10-23*

Abstract

Excessive radiation exposure may lead to edema of the spinal cord and deterioration of the nervous system. Magnetic resonance imaging can be used to judge and assess the extent of edema and to evaluate pathological changes and thus may be used for the evaluation of spinal cord injuries caused by radiation therapy. Radioactive ^{125}I seeds to irradiate 90% of the spinal cord tissue at doses of 40–100 Gy (D90) were implanted in rabbits at T_{10} to induce radiation injury, and we evaluated their safety for use in the spinal cord. Diffusion tensor imaging showed that with increased D90, the apparent diffusion coefficient and fractional anisotropy values were increased. Moreover, pathological damage of neurons and microvessels in the gray matter and white matter was aggravated. At 2 months after implantation, obvious pathological injury was visible in the spinal cords of each group. Magnetic resonance diffusion tensor imaging revealed the radiation injury to the spinal cord, and we quantified the degree of spinal cord injury through apparent diffusion coefficient and fractional anisotropy.

Key Words: *nerve regeneration; brachytherapy; ^{125}I radioactive seeds; magnetic resonance imaging; radiation injury of the spinal cord; diffusion tensor imaging; apparent diffusion coefficient; fractional anisotropy; neural regeneration*

Introduction

Spinal metastasis is the most common bone metastasis, and 70% of spinal metastases occur in the thoracic segment (Aydinli et al., 2006). In recent years, brachytherapy with ^{125}I radioactive seeds has been widely used in the treatment of a variety of malignant tumors (Jiang et al., 2010; Xiang et al., 2015; Yorozu et al., 2015; Shi et al., 2016; Song et al., 2017). There are also related studies and reports on the treatment of spinal metastases (Rogers et al., 2002; Zhang et al., 2013c; Liu et al., 2014; Yao et al., 2016; Yu et al., 2016). Brachytherapy with ^{125}I radioactive seeds is characterized by a small irradiated area and a concentrated killing effect on tumor tissue (Wang et al., 2010a). The number of ^{125}I seeds implanted in the metastatic site ranges from approximately 10 to dozens (Bilsky et al., 2004; Huang et al., 2004; Wieners et al., 2006; Wright et al., 2006; Yang et al., 2009; Feng et al., 2015). The spinal cord is less resistant to irradiation than other tissues, so excessive exposure may cause tissue edema and deteriorate neurological symptoms (Kirkpatrick et al., 2010). How to select appropriate numbers of radioactive seeds but avoid radiation injury to the spinal cord, to obtain the greatest killing effect deserves our in-depth study (Guan et al., 2016). However, data on brachytherapy for spinal metastases are limited, and only a few studies concern the safety issues for the spinal cord (Wang et al., 2013; Lu et al., 2015).

This study sought to observe spinal cord function through behavior, diffusion tensor imaging (DTI) and spinal cord neuropathology after irradiation with different doses for 90% spinal cord tissue (D90) values of ^{125}I radioactive seeds in the rabbit spinal cord. We investigated the application of DTI to assess radiation injury to the spinal cord and analyzed dynamic changes in DTI parameters and their relationship with limb function and spinal cord pathology.

Materials and Methods

^{125}I seeds

Radioactive ^{125}I seeds were provided by China Isotope & Radiation Corporation, China National Nuclear Corporation. Precise parameters were: closed ^{125}I radionuclide source, 4.5 mm × φ0.8 mm cylinder, 27.4–31.5 keV γ source, half-life of 59.6 days, tissue penetration capacity of 1.7 cm, and half value thickness of 0.025 mm lead. The surface was wrapped with titanium alloy. The initial dose rate was 0.13 Gy/min. One week later, the cumulative dose was higher than the conventional accelerator does of 10 Gy.

Determination of radiation dosimetry

A 5-mm-thick computed tomography (CT) scan was performed a week before ^{125}I brachytherapy in all rabbits. These images were imported to a Treatment Planning System (Brachy Pro v3.02, Fei Tian Zhao Ye Technology Co., Ltd., Beijing, China) to determine the dose of radioactive seeds to be implanted at the site. The paravertebral soft tissue of the non-transverse plane of the thoracic 10 (T_{10}) vertebra was set as the hypothetical tumor region. A careful delineation of the gross tumor volume and surrounding vital organs was made in every CT slice. The prescription dose for the "hypothetical tumor" was 80 Gy. At the same CT levels, D90 was 40, 60, 80 and 100 Gy in the different groups (**Figures 1** and **2**).

Animals

All surgical procedures and postoperative care were performed in accordance with the guidelines of the Institutional Animal Care and Use Committee of Jilin University, China (approval No. 20150625). Thirty-two clean adult New Zealand rabbits of both sexes (50% each), at the age of 1–1.5 years and weighing 3.5–4.5 kg were provided by Medical Laboratory Animal Center, Jilin University, China (license No. SCXK (Ji) 2013-0002). Their diet, exercise, reactions and urination were normal. Rabbits were acclimated for one week before model establishment.

By using randomization, self-pairing, and double-blind methods, rabbits were equally divided into four groups according to D90: 40 Gy, 60 Gy, 80 Gy and 100 Gy groups, with eight rabbits in each group. The 0.8 mCi ^{125}I seeds were implanted at T_{10} next to the vertebral lamina. Rabbits were executed by euthanasia on schedule and their spinal cords were aseptically removed for pathological observation.

Radioactive ^{125}I seed implantation next to the vertebral lamina

Rabbits were acclimated and fed with complete feed and tap water. Their eating and activities were observed. After fasting for 12 hours and water deprivation for 6 hours, rabbits were weighed and a CT scan was performed. The dose was calculated using the Treatment Planning System before surgery. The D90 on the test areas were 40, 60, 80 and 100 Gy. Rabbits were anesthetized with 10% chloral hydrate through the ear vein, and fixed on the table. After shaving, sterilizing with povidone iodine, and draping the rabbits, physicians wore lead glasses, lead gloves, a lead scarf and lead protective clothing, and contact time was minimized during implantation. Seeds were implanted at T_{10} next to the vertebral lamina according to the Treatment Planning System plan. CT scans and the Treatment Planning System were utilized for verification during and after surgery. Thus, the actual number of implanted seeds met the designed range of D90 ± 5% (**Figures 1** and **2**). After surgery, rabbits underwent intramuscular injection of penicillin (400,000 U) for 3 consecutive days.

Behavioral observation of spinal cord nerve injury

Rabbits in each group were housed under the same conditions. After seed implantation, behaviors were observed, recorded and scored once a week. Previous studies have evaluated motor function in spinal cord injury models using the Basso, Beattie and Bresnahan (BBB) locomotor scale and the oblique plate test, which cannot fully reflect the changes in animal models after radioactive spinal cord injury for aspects of exercise, sensation, and urination. In this study, according to a previous method (Song et al., 2004), the scoring criteria were set as follows:

(1) Motor function: (A) No abnormality; (B) incomplete paralysis: limited movement, walking but no jumping, hind

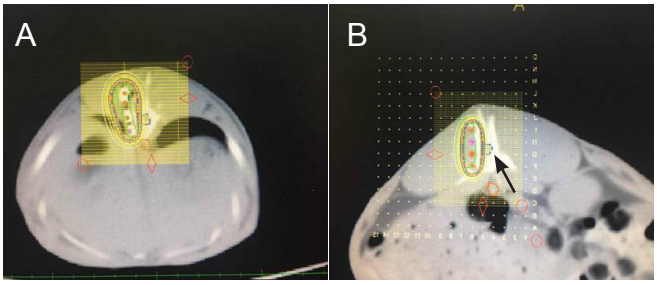

Figure 1 Rabbit with D90 brachytherapy of 60 Gy.
(A) Plan before seed implantation: The red dots are the projected sites of seed implantation. They appear orange when overlapped with the yellow coordinate points. (B) Verification after seed implantation: The red dots are the actual sites of seed implantation. The red arrow shows the spinal cord. D90: Doses for 90% spinal cord tissue.

limb trembling; (C) paralysis: hind limbs cannot move. A = 3 points; B = 2 points; C = 1 point.
(2) Hind limb pain sensation: pain response of the hind limbs after stimulation with a needle. (A) Normal response; (B) reduced response; (C) no response. A = 3 points; B = 2 points; C = 1 point.
(3) Urination: (A) Normal; (B) urine retention: if urine retention occurred, the urinary bladder was gently squeezed until urination, otherwise a urethral catheter was used. A = 3 points; B = 1 point.

Magnetic resonance detection

Magnetic resonance imaging (MRI) and DTI were conducted with a GE 1.5T Signa TwinSpeed MR system (Waukesha, WI, USA). MRI took coils on the surface of the knee as radiofrequency transmitting and receiving coils. T_{10} was considered as the center of the scanner field. T2 weighted imaging (T2WI), diffusion weighted imaging (DWI), and DTI sequences on the horizontal axis were performed. Scan parameters: horizontal axis of T2WI, FRFSE-XL, repetition time/echo time (TR/TE): 3,000/101.8 ms, field of view (FOV): 180 × 144 mm², slice thickness: 3.0 thk/0.5 sp, NEX: 4.00. DTI, spin echo-echo planar imaging (SE/EPI), TR/TE: 4,000/105.0 ms, FOV: 240 × 240 mm², slice thickness: 3.0 thk/0.5 sp, NEX: 4.00, b value: 600 s/mm², 16 diffusion gradient directions. DWI, SE/EPI, TR/TE: 4,000/62.4 ms, FOV: 260 × 195 mm², slice thickness: 3.0 thk/0.5 sp, NEX: 8.00, b value: 600 s/mm².

Images were processed with a GE AW4.2 workstation. DWI and DTI data were processed with Functool software. Hand-drawn regions of interest were measured (9–11 mm²). Each region was measured three times, and the average value was calculated. Cerebrospinal fluid artifacts were avoided during measurement where possible. Apparent diffusion coefficient (ADC) and fractional anisotropy (FA) values were obtained. Foci were analyzed by two experienced physicians. Imaging changes in the spinal cord were observed in a 6 cm range from seed implantation (upper 3 cm to lower 3 cm).

Neuropathological observation of the spinal cord

At 2 and 4 months after ^{125}I radioactive seed implantation, one rabbit from each group was sacrificed. All rabbits were sacrificed at 6 months for pathological observation. A total of

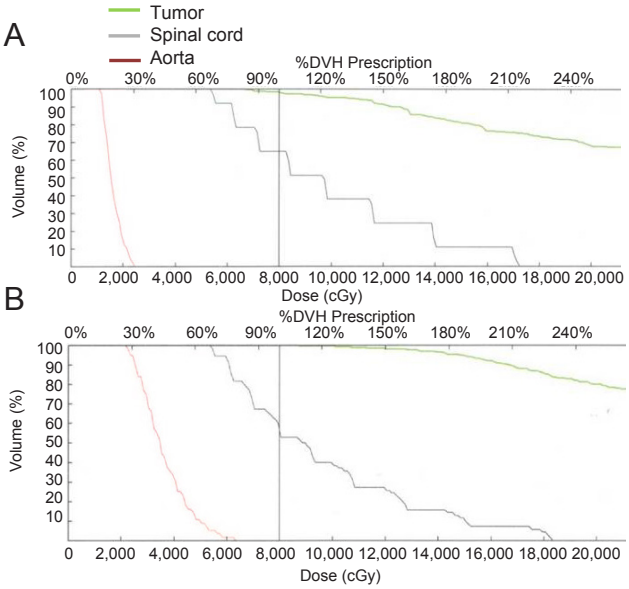

Figure 2 Real dose intensity of D90.
Dose-volume histograms (DVH) for the number 2 rabbit in the 60 Gy group. (A) The prescription dose was 80 Gy during the planning. A total of D90 received 61.8 Gy. The D90 was 11.5 Gy in the aorta. (B) After ^{125}I seed implantation, the dose intensity was verified; the D90 was 60.8 Gy and 24.1 Gy in spinal cord and aorta, respectively. D90: Doses for 90% spinal cord tissue.

50 mL of air was infused through an ear vein. Using CT, the position of the seeds was fixed with a needle. After exposure of the spinal cord, 6 cm of spinal cord containing the seeds was harvested as the radiation area for pathological observation. Spinal cord 2 cm proximal was used as a control to observe the pathological changes in normal spinal cord.

The spinal cord was cut into blocks and fixed in pre-formulated fixative. Thus, tissue and cell proteins were denatured and solidified to prevent cell autolysis or decomposition by bacteria after cell death, and to maintain the original morphological structure of the cells. Specimens were dehydrated with alcohol from a low concentration to a high concentration, treated with xylene, embedded in wax, sliced into sections and slide-mounted. The sections were dried in a 45°C incubator and then stained with hematoxylin and eosin.

Histopathological changes were observed under a light microscope (Leica DM2500; Wetzlar, Hesse-Darmstadt, Germany), including the degree of tissue damage, inflammation, necrosis, edema and hemorrhage. Indicators for morphological changes were demyelination, vacuolar degeneration, microvascular changes and glial cell proliferation.

Statistical analysis

The data, expressed as the mean ± SD, were analyzed using the SPSS 13.0 software (SPSS Inc., Chicago, IL, USA), using repeated measures analysis of variance. Paired comparisons were conducted using the least significant difference test. A value of $P < 0.05$ was considered statistically significant.

Results

Behavioral observation of spinal cord injury

Rabbits in each group were housed under the same condi-

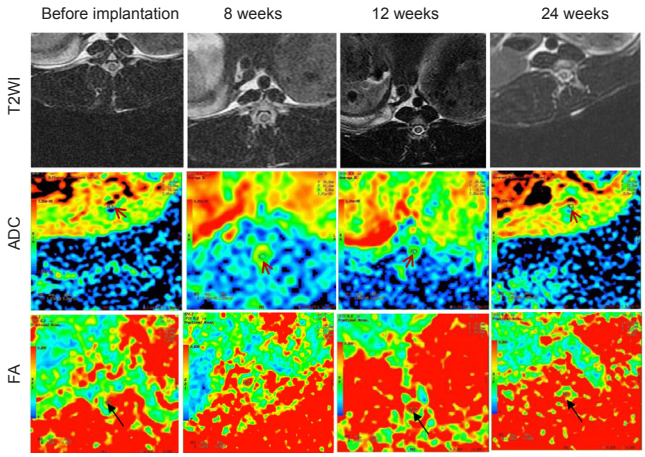

Figure 3 ADC (red arrows) and FA (black arrows) reconstruction of spinal cord in radiation injury rabbits at different time points after implantation.
Radioactive seeds were implanted in the tenth thoracic vertebra of rabbits in the 100 Gy group. The anatomical location of the spinal cord was identified according to T2 weighted imaging. ADC: Apparent diffusion coefficient; FA: fractional anisotropy.

Table 1 Clinical symptoms of rabbits in each group at various time points after ^{125}I seed implantation

Group	Motor function changes	Pain sensation changes	Urine retention	Score
40 Gy				
0–8 weeks	0/8	0/8	0/8	9±0
9–10 weeks	0/7	0/7	0/7	9±0
12 weeks	0/7	0/7	0/7	9±0
16 weeks	0/6	0/6	0/6	9±0
20 weeks	0/6	0/6	0/6	9±0
24 weeks	0/6	1/6	0/6	8.83±0.41
60 Gy				
0–8 weeks	0/8	0/8	0/8	9±0
9–10 weeks	0/7	0/7	0/7	9±0
12 weeks	0/7	0/7	0/7	9±0
16 weeks	0/6	0/6	0/6	9±0
20 weeks	0/6	1/6	0/6	8.83±0.41
24 weeks	0/6	1/6	0/6	8.83±0.41
80 Gy				
0–8 weeks	0/8	0/8	0/8	9±0
9–10 weeks	0/7	0/7	0/7	9±0
12 weeks	0/7	0/7	0/7	9±0
16 weeks	0/6	1/6	0/6	8.83±0.41
20 weeks	0/6	1/6	0/6	8.83±0.41
24 weeks	0/6	1/6	0/6	8.83±0.41
100 Gy				
0–8 weeks	0/8	0/8	0/8	9±0
9–10 weeks	0/7	0/7	0/7	9±0
12 weeks	0/7	0/7	0/7	9±0
16 weeks	0/6	1/6	0/6	8.83±0.41
20 weeks	0/6	1/6	1/6	8.50±0.84
24 weeks	1/6	2/6	2/6	7.67±0.82

Data on motor function changes, pain sensation changes and urine retention represent the number of animals with positive symptoms/total number of animals. The score value is expressed as the mean ± SD.

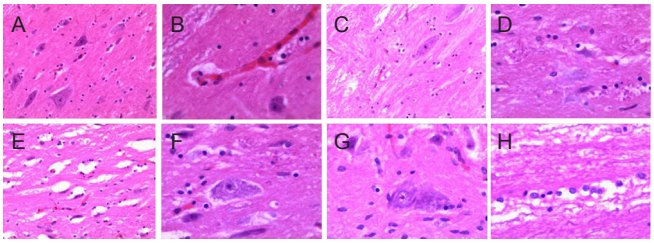

Figure 4 Pathological changes in the spinal cord in radiation injury rabbits after ^{125}I radiative seed implantation (hematoxylin-eosin staining).
(A) The nuclei of neurons in the spinal cord were large, round and centrally located on the control side at 6 months after ^{125}I seed irradiation. Axons and axon hillocks displayed dendrites that extended from the upper right of the cell, and glial nuclei were found between dendrites and axons. (B) Spinal microvascular changes on the control side at 6 months after ^{125}I seed irradiation. (C) Glial cells around spinal cord neurons on the control side at 6 months after ^{125}I seed irradiation. (D) Neuronal disintegration and necrosis of the anterior horn of the spinal cord, with vague contours of residual cells and karyolysis, and disappearance of Nissl bodies in the cytoplasm at 4 months after ^{125}I seed irradiation. (E) Microvascular proliferation and local endothelial cell swelling at 2 months after ^{125}I seed irradiation. (F) Fuzzy neuron nuclear membrane, vacuolar nucleus degeneration, and perinuclear halo at 4 months after ^{125}I seed irradiation. (G) Nuclear vacuolar degeneration, Nissl body degeneration, peripheral glial cell proliferation, and destruction of neurons by phagocytic cells at 6 months after ^{125}I seed irradiation. (H) Axonal degeneration and disintegration, significant glial cell proliferation, and myelinated nerve fiber demyelination at 6 months after ^{125}I seed irradiation. Original magnification: 200× in A, C, E and 400× in B, D, F–H.

tions. After seed implantation, behaviors were observed. Clinical performance scores were significantly lower in the 100 Gy group than in the 40 Gy, 60 Gy and 80 Gy groups 6 months after ^{125}I seed implantation (7.67 ± 0.82 (100 Gy group) *vs.* 8.83 ± 0.41 (40 Gy group, 60 Gy group, 80 Gy group); $F = 7.000$, $P < 0.05$). Rabbits in the 40 Gy and 60 Gy groups displayed normal physiological activities and motor functions were not affected. However, at 5 months, pain sensitivity in response to needle stimulation decreased in one rabbit in the 60 Gy group, and at 6 months, pain sensitivity decreased in one rabbit in the 40 Gy group. In the 80 Gy group, rabbits showed normal physiological activities, decreased pan sensitivity and diminished eating, but motor function was good in one rabbit at 4 months. In the 100 Gy group, rabbits were normal for the first three months but pain sensitivity decreased and urine retention appeared in some rabbits at 4, 5 and 6 months. By the end of the experiment one rabbit suffered from dyskinesia-induced incomplete paralysis (**Table 1**). The above findings confirmed that with increased D90, motor function and pain sensitivity gradually diminished and when the D90 was 100 Gy, spinal cord function was noticeably impaired.

DTI observation

T2WI and DTI sequences were performed preoperatively, and at 2, 4, 6, 8, 10, 12, 16, 20, and 24 weeks postoperatively. Imaging changes in the spinal cord were observed in the 6 cm range of seed implantation (upper 3 cm to lower 3 cm). ADC and FA values were obtained in the range of seed irradiation.

Table 2 Comparison of apparent diffusion coefficient ($\times 10^{-3}$ mm/s^2) in the rabbit spinal cord at various time points after seed implantation

	40 Gy group	60 Gy group	80 Gy group	100 Gy group
Preoperatively	1.142±0.193	1.116±0.184	1.142±0.173	1.135±0.203
Postoperatively				
2 weeks	1.177±0.230	1.169±0.221	1.167±0.236	1.178±0.214
4 weeks	1.215±0.245	1.233±0.304	1.225±0.265	1.237±0.242##
6 weeks	1.224±0.221	1.262±0.244	1.343±0.224	1.326±0.273##
8 weeks	1.308±0.219	1.340±0.283	1.352±0.306	1.412±0.285##
10 weeks	1.382±0.254	1.397±0.265#	1.431±0.291#	1.461±0.316##
12 weeks	1.303±0.263	1.352±0.251#	1.405±0.253#	1.453±0.263##
16 weeks	1.295±0.246	1.348±0.250#	1.362±0.272	1.395±0.228##
20 weeks	1.266±0.252	1.335±0.218#	1.311±0.246	1.334±0.184##
24 weeks	1.261±0.231	1.272±0.249	1.283±0.195	1.319±0.211##

Data are expressed as the mean ± SD and were analyzed by repeated measures analysis of variance; #$P < 0.05$, ## $P < 0.01$, *vs*. preoperatively.

Table 3 Comparison of fractional anisotropy values in the rabbit spinal cord at various time points after seed implantation

	40 Gy group	60 Gy group	80 Gy group	100 Gy group
Preoperatively	1.142±0.193	1.116±0.184	1.142±0.173	1.135±0.203
Postoperatively				
4 weeks	0.618±0.031	0.62±0.026	0.622±0.028	0.618±0.027
6 weeks	0.617±0.022	0.628±0.031	0.618±0.031	0.613±0.032
8 weeks	0.605±0.027	0.621±0.022	0.611±0.026	0.608±0.024
10 weeks	0.603±0.025	0.613±0.026	0.605±0.024	0.609±0.028
12 weeks	0.592±0.019	0.606±0.031	0.596±0.029	0.586±0.022#
16 weeks	0.578±0.025	0.595±0.024	0.593±0.031	0.584±0.023#
20 weeks	0.594±0.023	0.594±0.029	0.584±0.028#	0.576±0.030#
24 weeks	0.585±0.024	0.588±0.035	0.588±0.027#	0.577±0.026#

Data are expressed as the mean ± SD and analyzed by repeated measures analysis of variance; #$P < 0.05$, *vs*. preoperatively.

Repeated measures analysis of variance compared ADC values at various times points ($F = 7.536$, $P < 0.001$) in each dose group ($F = 0.294$, $P = 0.829$). Repeated measures analysis of variance also compared the FA values at various time points ($F = 11.916$, $P < 0.001$) in each dose group ($F = 1.441$, $P = 0.252$). Results are shown in **Tables 2** and **3**, and **Figure 3**.

In each group, the T2WI sequence did not reveal abnormal spinal cord morphology or signal. DTI demonstrated an alteration in ADC values in the 60 Gy, 80 Gy and 100 Gy groups. With prolonged time after implantation, ADC values gradually increased and were significantly different at 10 weeks postoperatively compared with preoperatively in the 60 Gy and 80 Gy groups ($P < 0.05$). ADC values were significantly different at 4 weeks postoperatively until the end of the experiment compared with preoperatively in the 100 Gy group ($P < 0.05$). ADC values gradually reduced, but were still higher than preoperatively, and with increased D90, ADC values were increased.

The changes in FA values were not as remarkable as the ADC values. With prolonged time, FA values decreased, beginning to diminish at about 12 weeks until the end of the experiment in the 100 Gy group ($P < 0.05$, *vs*. preoperatively). In the 80 Gy group FA values began to significantly decrease at about 20 weeks compared with preoperative values ($P < 0.05$).

Neuropathological observation of the spinal cord

Results of hematoxylin-eosin staining showed that the number of neuronal cells in the gray matter of the spinal cord was reduced and some neurons were damaged in the 40 Gy and 60 Gy groups. The neuronal cell loss increased, the nuclear membrane was blurred in some neurons, and some cells were damaged in the 80 Gy group. In the 100 Gy group, there was neuronal demyelination, pyknosis, cytoplasmic eosinophilic changes, cytolysis, cell disappearance, ghost cells, and cyst formation. Early changes in the white matter of the spinal cord included microvascular changes, edema and exudation around blood vessels. The white matter presented nerve fiber swelling, demyelination, degeneration, and disintegration. At 2 months after implantation, the main microvascular changes included microvascular dilation, vascular endothelial cell swelling, and microvascular disorder. At 4–6 months, edema and exudation around microvessels, and a sparse microvascular distribution were visible in the irradiated area. The above changes suggested that pathological damage of the spinal cord was increased with increased D90 (**Figure 4**).

Discussion

Brachytherapy with ^{125}I radioactive seeds is the application of atomic physics to clinical medicine. Implantation of ^{125}I

seeds is a new kind of treatment method for tumors and is complementary to surgery and external radiotherapy. Under the surveillance of B ultrasound and CT, ^{125}I radioactive seeds are implanted for persistent radiation therapy of tumors using a puncture technique. This method is characterized by a small amount of trauma, a precise target center, and low-dose sustained gamma radiation (Guan et al., 2016). The activity of ^{125}I is low and the penetration force is weak, so it is easy to protect other tissues with brachytherapy. Spinal metastasis is one of the most common complications of cancer. At present, ^{125}I seeds are used to treat spinal metastases but the evaluation and research of their safety are relatively lagging. Tolerance of the spinal cord to radioactive ^{125}I seeds and the effects of excess radiation on spinal cord injury remain poorly understood. In particular, there is a lack of large-sample randomized controlled trials. It is unclear how to avoid radiation injury to the spinal cord yet obtain a high tumor control rate. The main contraindication is that the spinal cord is not very resistant to radiation, so excessive exposure may cause tissue edema, resulting in neurological deterioration.

Previous studies on radiation injury to the spinal cord have investigated the tolerance dose and the short-term and long-term pathological changes of the spinal cord. However, the premise of the studies was constant dose irradiation with Body Gamma Knife (Yu et al., 2000) or a linear accelerator (Medin et al., 2012). The pathological changes of the spinal cord were analyzed and studied according to different irradiation doses. Radioactive ^{125}I seed therapy is characterized by small-range, continuous uniform irradiation after implantation, which is different from conventional radiotherapy (Wang et al., 2010b; Liu et al., 2011). This study established rabbit models implanted with ^{125}I radioactive seeds, investigated the application of DTI to assess radiation injury, and analyzed dynamic changes of DTI parameters and their relationship with limb function and pathology.

Our results showed that spinal cord microvessels of all specimens were altered, mainly presenting microvascular dilation and vascular endothelial cell swelling. The number of microvessels was noticeably increased, but vascular morphology was different from normal blood vessels, mainly presenting microvascular disorder. This is not the same as reported in a study of single irradiation-induced injury to the spinal cord, indicating that the mechanism of radiation injury to the spinal cord induced by ^{125}I seeds is different from that of conventional radiotherapy (Zhang et al., 2013b). In the middle and late stages of the experiment, edema and exudation around microvessels, and sparse microvascular distribution were seen in the irradiated area. The degree of neuronal damage was different among groups. Some neurons were enlarged or lost in the 40 Gy and 60 Gy groups. The proportion of neuronal loss was increased and the nuclear membrane was obscure in the 80 Gy group. Pyknosis, cytoplasmic eosinophilic changes, cytolysis, cell disappearance, ghost cells and cyst formation were observed in the 100 Gy group. Pathological observation demonstrated that microvessels, especially vascular endothelium, were most sensitive to seed irradiation. Vascular endothelial cell swelling was found in the early stage. The early changes of the white matter of the spinal cord mainly involved the changes of microvessels, edema, and exudation around the microvessels. The white matter showed nerve fiber swelling and demyelination, degeneration and disintegration. Simultaneously, neuronal swelling, degeneration, and cyst formation were visible. This is not consistent with a previous study (Zhang et al., 2013a) in a model of single irradiation-induced injury to the spinal cord, which reported that the number of neurons was significantly decreased in the early stage after irradiation. The above findings suggest that the mechanism of radiation injury to the spinal cord induced by ^{125}I seeds is different from that of conventional radiotherapy.

Radiation injury to the spinal cord has been classified into three types (Schultheiss et al., 1990): type I, only involving white matter or slight vascular changes, not enough to produce symptoms; type II, vascular changes that can cause secondary change to the white matter; type III, white matter and blood vessels are damaged. In accordance with pathogenesis and pathological characteristics of radiation injury to the spinal cord, magnetic resonance can be used to assess the extent of edema (Kerkovský et al., 2012; Jirjis et al., 2013), the damage of fiber bundles (Kozlowski et al., 2008; Mohamed et al., 2011; Gasparotti et al., 2013; Naismith et al., 2013; Yin et al., 2014) or the continuity of their distribution (Hobert et al., 2013; Koskinen et al., 2013; Ulmer et al., 2014; Patel et al., 2016), and areas of vascular injury or bleeding (Shanmuganathan et al., 2008; Chalian et al., 2011). Therefore, T2WI and DTI can be used as effective sequences for the evaluation of radiation injury to the spinal cord. DTI is a magnetic resonance imaging technique that measures the restricted diffusion of water in tissue, and is a noninvasive technique. Thus, the application of this method to evaluate the changes in the spinal cord has unique characteristics and advantages (Gao et al., 2013; Mondragon-Lozano et al., 2013; Mulcahey et al., 2013; Ohn et al., 2013; Jang and Seo, 2015; Kim et al., 2015; Ouyang et al., 2015). Many previous studies focused on mechanical damage and radiation injury to the spinal cord (Ratanatharathorn et al., 1999; Li et al., 2016). The functional recovery of the spinal cord was assessed by comparing the changes in ADC and FA values preoperatively and postoperatively (Kim et al., 2010; Zhang et al., 2015). Previous studies also showed the changes in the nervous system evaluated by DTI after radiotherapy. Nevertheless, few studies have addressed the changes in the spinal cord after ^{125}I seed implantation around vertebral bodies. The radiation characteristics and manner of use of radioactive seeds in the spinal cord are different from those of conventional radiotherapy, so the effects of ^{125}I seeds on the spinal cord deserve further investigation and evaluation (Medin and Boike, 2011).

Our results showed that ADC values altered in each group. With prolonged time of implantation, ADC values gradually increased and were significantly different at 10 weeks postoperatively compared with preoperatively in the 60 Gy and 80 Gy groups. ADC values were significantly different at 4 weeks postoperatively until the end of the

experiment compared with preoperatively in the 100 Gy group. The above findings indicated that the spinal cord had an early injury at 4 or 10 weeks. Pathological changes demonstrated microvascular dilation, vascular endothelial cell swelling, and microvascular disorder in the spinal cord at 1 and 2 months. Therefore, the changes in ADC values mainly reflected the changes in spinal cord microvessels. During this period, FA values did not change significantly, indirectly reflecting that the white matter fiber distribution did not change remarkably. With prolonged time, FA values were decreased, and began to diminish from about 12 weeks until the end of the experiment in the 100 Gy group. In the 80 Gy group, FA values began to decrease at about 20 weeks, and were significantly different between 20 weeks postoperatively compared with preoperatively. Pathological analysis revealed edema and exudation around microvessels, and a sparse microvascular distribution was visible in the irradiated area in the middle and late stages of the experiment. Glial cell proliferation was seen in the 100 Gy group. Therefore, we believed that the decrease in FA values was associated with the changes in fiber tracts within the white matter at the irradiated area, which is consistent with a previous study (Zhao et al., 2016), possibly because perivascular exudation or gliosis caused changes in the structure of fiber tracts within the white matter, thereby resulting in limb and spinal cord dysfunction. Our results also demonstrated that clinical performance scores were significantly lower in the 100 Gy group than in the 40 Gy, 60 Gy and 80 Gy groups 6 months after ^{125}I seed implantation. When the D90 was 100 Gy, spinal cord function was noticeably impaired. The time of this change is basically consistent with the time point of the FA change, suggesting that the change of FA value may be associated with the appearance of clinical symptoms.

In conclusion, ^{125}I radioactive seed implantation next to the vertebral lamina in rabbits for 2 months can result in microvascular dilation and vascular endothelial cell swelling and may develop into radiation injury of the spinal cord. The degree of injury increased with increasing D90. Magnetic resonance DTI sequencing can sensitively detect early radiation injury and has the advantage that it can display the state and structure of the white matter fibers in the spinal cord. DTI sequencing can also assess the degree of radiation injury through the changes in ADC and FA values, is useful for the evaluation of spinal cord changes after seed implantation, and quantifies the number of implanted seeds in the treatment of malignant tumors. However, this study is only a preliminary exploration of the possible effects of ^{125}I seeds on spinal cord injury. Because of the small sample size, it cannot fully reflect the changes of the spinal cord. Because of the magnetic field intensity, this study cannot accurately describe the changes of the white and gray matter of the spinal cord. With the limitation of observation time, the long-term changes of the spinal cord after irradiation could not be provided. These problems need to be further studied in future research.

Author contributions: *TWW conceived and designed the study. XC carried out the data collection, prepared the figures, and drafted the paper. LF and CYC participated in the data collection. CYC carried out the needle penetration. TWW and CYC were responsible for seeds implantation. SG and TWW carried out the dose calculation of seeds implantation. All authors read and approved the final version of the paper.*
Conflicts of interest: *None declared.*
Financial suppport: *This study was supported by the Science and Technology Development Project Funds of Science and Technology Department of Jilin Province in China, No. 20120724. The funder had no involvement in the study design; data collection, analysis, and interpretation; paper writing; or decision to submit the papaer for publication.*
Research ethics: *The study protocol was approved by the Institutional Animal Care and Use Committee of Jilin University, China (approval No. 20150625).*
Data sharing statement: *Datasets analyzed during the current study are available from the corresponding author on reasonable request.*
Plagiarism check: *Checked twice by iThenticate.*
Peer review: *Externally peer reviewed.*
Open access statement: *This is an open access article distributed under the terms of the Creative Commons Attribution-NonCommercial-ShareAlike 3.0 License, which allows others to remix, tweak, and build upon the work non-commercially, as long as the author is credited and the new creations are licensed under identical terms.*

References

Aydinli U, Ozturk C, Bayram S, Sarihan S, Evrensel T, Yilmaz HS (2006) Evaluation of lung cancer metastases to the spine. Acta Orthop Belg 72:592-597.

Bilsky MH, Yamada Y, Yenice KM, Lovelock M, Hunt M, Gutin PH, Leibel SA (2004) Intensity-modulated stereotactic radiotherapy of paraspinal tumors: a preliminary report. Neurosurgery 54:823-830; discussion 830-831.

Chalian M, Tekes A, Meoded A, Poretti A, Huisman TA (2011) Susceptibility-weighted imaging (SWI): a potential non-invasive imaging tool for characterizing ischemic brain injury? J Neuroradiol 38:187-190.

Feng S, Wang L, Xiao Z, Maharjan R, Chuanxing L, Fujun Z, Jinhua H, Peihong W (2015) ^{125}I seed implant brachytherapy for painful bone metastases after failure of external beam radiation therapy. Medicine (Baltimore) 94:e1253.

Gao SJ, Yuan X, Jiang XY, Liu XX, Liu XP, Wang YF, Cao JB, Bai LN, Xu K (2013) Correlation study of 3T-MR-DTI measurements and clinical symptoms of cervical spondylotic myelopathy. Eur J Radiol 82:1940-1945.

Gasparotti R, Lodoli G, Meoded A, Carletti F, Garozzo D, Ferraresi S (2013) Feasibility of diffusion tensor tractography of brachial plexus injuries at 1.5 T. Invest Radiol 48:104-112.

Guan J, Yuan ZC, Liu B (2016) Research progress of ^{125}I seeds implantation for metastatic spinal tumors. Zhonghua Zhongliu Fangzhi Zazhi 23:1392-1397.

Hobert MK, Stein VM, Dziallas P, Ludwig DC, Tipold A (2013) Evaluation of normal appearing spinal cord by diffusion tensor imaging, fiber tracking, fractional anisotropy, and apparent diffusion coefficient measurement in 13 dogs. Acta Vet Scand 55:36.

Huang ZG, Zhang XZ, Wang W, Luo XL, Wang JY (2004) CT-guided percutaneous permanent ^{125}I implantation for patients with malignant tumor. Zhonghua Fangshe Xue Zazhi 38:921-925.

Jang SH, Seo JP (2015) Aging of corticospinal tract fibers according to the cerebral origin in the human brain: a diffusion tensor imaging study. Neurosci Lett 585:77-81.

Jiang YL, Meng N, Wang JJ, Jiang P, Yuan H, Liu C, Qu A, Yang RJ (2010) CT-guided iodine-125 seed permanent implantation for recurrent head and neck cancers. Radiat Oncol 5:68.

Jirjis MB, Kurpad SN, Schmit BD (2013) Ex vivo diffusion tensor imaging of spinal cord injury in rats of varying degrees of severity. J Neurotrauma 30:1577-1586.

Kerkovský M, Bednarík J, Dušek L, Sprláková-Puková A, Urbánek I, Mechl M, Válek V, Kadanka Z (2012) Magnetic resonance diffusion tensor imaging in patients with cervical spondylotic spinal cord compression: correlations between clinical and electrophysiological findings. Spine (Phila Pa 1976) 37:48-56.

Kim JH, Loy DN, Wang Q, Budde MD, Schmidt RE, Trinkaus K, Song SK (2010) Diffusion tensor imaging at 3 hours after traumatic spinal cord injury predicts long-term locomotor recovery. J Neurotrauma 27:587-598.

Kim SY, Shin MJ, Chang JH, Lee CH, Shin YI, Shin YB, Ko HY (2015) Correlation of diffusion tensor imaging and phase-contrast MR with clinical parameters of cervical spinal cord injuries. Spinal Cord 53:608-614.

Kirkpatrick JP, van der Kogel AJ, Schultheiss TE (2010) Radiation dose-volume effects in the spinal cord. Int J Radiat Oncol Biol Phys 76:S42-49.

Koskinen E, Brander A, Hakulinen U, Luoto T, Helminen M, Ylinen A, Ohman J (2013) Assessing the state of chronic spinal cord injury using diffusion tensor imaging. J Neurotrauma 30:1587-1595.

Kozlowski P, Raj D, Liu J, Lam C, Yung AC, Tetzlaff W (2008) Characterizing white matter damage in rat spinal cord with quantitative MRI and histology. J Neurotrauma 25:653-676.

Li XF, Yang Y, Lin CB, Xie FR, Liang WG (2016) Assessment of the diagnostic value of diffusion tensor imaging in patients with spinal cord compression: a meta-analysis. Braz J Med Biol Res 49:e4769.

Liu C, Wang JJ, Meng N, Liu XG, Jiang LX, Ma YQ, Han CB, Yuan HS (2011) CT-guide interstitial iodine-125 seed implantation for metastatic spine tumor. Zhongguo Jizhu Jisui Zazhi 21:226-229.

Liu JL, Gao GY, Zhen WX, Liu Y, Yang DZ, Lin EH (2014) Iodine-125 radioactive seed implantation combined with vertebroplasty and nail-rod fixation for thoracolumbar metastatic tumors. Zhongguo Zuzhi Gongcheng Yanjiu 18:4200-4205.

Lu J, Zhang LY, Wang ZM, Teng GJ, Chen KM, Chen ZJ, Gong J (2015) ^{125}I radioactive seed interstitial brachytherapy for the treatment of metastatic epidural spinal cord compression. Jieru Fangshe Xue Zazhi 24:693-697.

Medin PM, Boike TP (2011) Spinal cord tolerance in the age of spinal radiosurgery: lessons from preclinical studies. Int J Radiat Oncol Biol Phys 79:1302-1309.

Medin PM, Foster RD, van der Kogel AJ, Sayre JW, McBride WH, Solberg TD (2012) Spinal cord tolerance to reirradiation with single-fraction radiosurgery: a swine model. Int J Radiat Oncol Biol Phys 83:1031-1037.

Mohamed FB, Hunter LN, Barakat N, Liu CS, Sair H, Samdani AF, Betz RR, Faro SH, Gaughan J, Mulcahey MJ (2011) Diffusion tensor imaging of the pediatric spinal cord at 1.5T: preliminary results. AJNR Am J Neuroradiol 32:339-345.

Mondragon-Lozano R, Diaz-Ruiz A, Rios C, Olayo Gonzalez R, Favila R, Salgado-Ceballos H, Roldan-Valadez E (2013) Feasibility of in vivo quantitative magnetic resonance imaging with diffusion weighted imaging, T2-weighted relaxometry, and diffusion tensor imaging in a clinical 3 tesla magnetic resonance scanner for the acute traumatic spinal cord injury of rats: technical note. Spine (Phila Pa 1976) 38:E1242-1249.

Mulcahey MJ, Samdani AF, Gaughan JP, Barakat N, Faro S, Shah P, Betz RR, Mohamed FB (2013) Diagnostic accuracy of diffusion tensor imaging for pediatric cervical spinal cord injury. Spinal Cord 51:532-537.

Naismith RT, Xu J, Klawiter EC, Lancia S, Tutlam NT, Wagner JM, Qian P, Trinkaus K, Song SK, Cross AH (2013) Spinal cord tract diffusion tensor imaging reveals disability substrate in demyelinating disease. Neurology 80:2201-2209.

Ohn SH, Kim DY, Shin JC, Kim SM, Yoo WK, Lee SK, Park CH, Jung KI, Jang KU, Seo CH, Koh SH, Jung B (2013) Analysis of high-voltage electrical spinal cord injury using diffusion tensor imaging. J Neurol 260:2876-2883.

Ouyang A, Jeon T, Sunkin SM, Pletikos M, Sedmak G, Sestan N, Lein ES, Huang H (2015) Spatial mapping of structural and connectional imaging data for the developing human brain with diffusion tensor imaging. Methods 73:27-37.

Patel SP, Smith TD, VanRooyen JL, Powell D, Cox DH, Sullivan PG, Rabchevsky AG (2016) Serial diffusion tensor imaging in vivo predicts long-term functional recovery and histopathology in rats following different severities of spinal cord injury. J Neurotrauma 33:917-928.

Ratanatharathorn V, Powers WE, Moss WT, Perez CA (1999) Bone metastasis: review and critical analysis of random allocation trials of local field treatment. Int J Radiat Oncol Biol Phys 44:1-18.

Rogers CL, Theodore N, Dickman CA, Sonntag VK, Thomas T, Lam S, Speiser BL (2002) Surgery and permanent ^{125}I seed paraspinal brachytherapy for malignant tumors with spinal cord compression. Int J Radiat Oncol Biol Phys 54:505-513.

Schultheiss TE, Stephens LC, Jiang GL, Ang KK, Peters LJ (1990) Radiation myelopathy in primates treated with conventional fractionation. Int J Radiat Oncol Biol Phys 19:935-940.

Shanmuganathan K, Gullapalli RP, Zhuo J, Mirvis SE (2008) Diffusion tensor MR imaging in cervical spine trauma. AJNR Am J Neuroradiol 29:655-659.

Shi L, Li X, Pei H, Zhao J, Qiang W, Wang J, Xu B, Chen L, Wu J, Ji M, Lu Q, Li Z, Wang H, Jiang J, Wu C (2016) Phase II study of computed tomography-guided (125)I-seed implantation plus chemotherapy for locally recurrent rectal cancer. Radiother Oncol 118:375-381.

Song J, Fan X, Zhao Z, Chen M, Chen W, Wu F, Zhang D, Chen L, Tu J, Ji J (2017) ^{125}I brachytherapy of locally advanced non-small-cell lung cancer after one cycle of first-line chemotherapy: a comparison with best supportive care. Onco Targets Ther 10:1345-1352.

Song T, Liang BL, Huang HQ, Mao YL, Liu YM, Cui NJ (2004) Treatment effect of neurotropin on radiation injury of spinal cord in rabbit's. Zhongguo Jizhu Jisui Zazhi 14:748-751.

Ulmer JL, Klein AP, Mueller WM, DeYoe EA, Mark LP (2014) Preoperative diffusion tensor imaging: improving neurosurgical outcomes in brain tumor patients. Neuroimaging Clin N Am 24:599-617.

Wang H, Wang JJ, Yuan HS, Liu XG, Zhu LH, Jiang YL, Yang RJ, Jiang WJ, Li JN, Tian SQ (2010a) ^{125}I seeds interstitial brachytherapy for vertebral and paraspinal carcinomas. Xiandai Zhongliu Yixue 18:146-148.

Wang HX, Huo XD, Shi KM, Zheng BS, Liu JZ, Zhang WY, Jiao L, Yang JK, Ma WT (2013) Study on the rat's dorsal root ganglion after ^{125}I brachytherapy. Zhonghua Fangshe Yixue yu Fanghu Zazhi 33:588-592.

Wang J, Yuan H, Ma Q, Liu X, Wang H, Jiang Y, Tian S, Yang R (2010b) Interstitial ^{125}I seeds implantation to treat spinal metastatic and primary paraspinal malignancies. Med Oncol 27:319-326.

Wieners G, Pech M, Rudzinska M, Lehmkuhl L, Wlodarczyk W, Miersch A, Hengst S, Felix R, Wust P, Ricke J (2006) CT-guided interstitial brachytherapy in the local treatment of extrahepatic, extrapulmonary secondary malignancies. Eur Radiol 16:2586-2593.

Wright JL, Lovelock DM, Bilsky MH, Toner S, Zatcky J, Yamada Y (2006) Clinical outcomes after reirradiation of paraspinal tumors. Am J Clin Oncol 29:495-502.

Xiang Z, Li G, Liu Z, Huang J, Zhong Z, Sun L, Li C, Zhang F (2015) ^{125}I Brachytherapy in locally advanced nonsmall cell lung cancer after progression of concurrent radiochemotherapy. Medicine (Baltimore) 94:e2249.

Yang Z, Yang D, Xie L, Sun Y, Huang Y, Sun H, Liu P, Wu Z (2009) Treatment of metastatic spinal tumors by percutaneous vertebroplasty versus percutaneous vertebroplasty combined with interstitial implantation of 125I seeds. Acta Radiol 50:1142-1148.

Yao L, Cao Q, Wang J (2016) CT-guided ^{125}I seed interstitial brachytherapy as a salvage treatment for recurrent spinal metastases after external beam radiotherapy. 2016:8265907.

Yin XY, Qiu SJ, Liu ZY, Wang HZ, Xiong WF, Li SS, Wang Y (2014) Extratemporal abnormalities of brain parenchyma in young adults with temporal lobe epilepsy: a diffusion tensor imaging study. Clin Radiol 69:589-596.

Yorozu A, Kuroiwa N, Takahashi A, Toya K, Saito S, Nishiyama T, Yagi Y, Tanaka T, Shiraishi Y, Ohashi T (2015) Permanent prostate brachytherapy with or without supplemental external beam radiotherapy as practiced in Japan: outcomes of 1300 patients. Brachytherapy 14:111-117.

Yu CL, Cui XJ, Cao GW, Du MM, Ning HF (2016) The clinical application of permanent implantation of ^{125}I seeds in treating metastatic bone pain. Jieru Fangshe Xue Zazhi 25:515-518.

Yu JM, Sun XD, Yang XH, Lu HJ, Lu H (2000) The research of spinal cord injury induced by body gamma knief. Zhongliu Fangzhi Zazhi 17:567-569.

Zhang D, Li XH, Zhai X, He XJ (2015) Feasibility of 3.0 T diffusion-weighted nuclear magnetic resonance imaging in the evaluation of functional recovery of rats with complete spinal cord injury. Neural Regen Res 10:412-418.

Zhang J, Wei LP, Sun WL, Zhang JG, You H, Zhang WJ (2013a) Regulation of number of neurons following radiation-induced spinal cord injury in rats. Xiandai Shengwu Yixue Jinzhan 13:1219-1222.

Zhang J, Wei LP, Sun WL, Zhang JG, You H, Zhang WJ (2013b) Regularity of spinal cord blood flow following radiation-induced spinal cord injury in rats. Xiandai Shengwu Yixue Jinzhan 13:2801-2803.

Zhang LY, Lu J, Gong J, Wang ZM, Zheng YF, Chen ZJ, Chen KM (2013c) Clinic efficacy of CT-guided ^{125}I seeds implantation therapy in patients with advanced vertebrae metastatic tumor. Shengwu Yixue Gongcheng yu Linchuang 17:147-151.

Zhao C, Rao JS, Pei XJ, Lei JF, Wang ZJ, Yang ZY, Li XG (2016) Longitudinal study on diffusion tensor imaging and diffusion tensor tractography following spinal cord contusion injury in rats. Neuroradiology 58:607-614.

(Copyedited by Turnley A, Maxwell R, Yu J, Li CH, Qiu Y, Song LP, Zhao M)